Efficient gold(III) detection, separation and recovery from urban mining waste using a facial conjugate adsorbent

ARTICLE *in* SENSORS AND ACTUATORS B CHEMICAL · JUNE 2014

Impact Factor: 4.1 · DOI: 10.1016/j.snb.2014.02.055

2 AUTHORS:

Md. Rabiul Awual
Japan Atomic Energy Agency
72 PUBLICATIONS **1,296** CITATIONS
SEE PROFILE

Mohamed Ismael
Sohag University
39 PUBLICATIONS **598** CITATIONS
SEE PROFILE

Sensors and Actuators B 196 (2014) 457–466

Contents lists available at ScienceDirect

Sensors and Actuators B: Chemical

journal homepage: www.elsevier.com/locate/snb

Efficient gold(III) detection, separation and recovery from urban mining waste using a facial conjugate adsorbent

Md. Rabiul Awual [a,*], Mohamed Ismael [b]

[a] Actinide Coordination Chemistry Group, Quantum Beam Science Directorate (QuBS), Japan Atomic Energy Agency (SPring-8), Hyogo 679-5148, Japan
[b] Department of Chemistry, Faculty of Science, Sohag University, Sohag-82524, Egypt

ARTICLE INFO

Article history:
Received 18 November 2013
Received in revised form 11 February 2014
Accepted 17 February 2014
Available online 23 February 2014

Keywords:
Ultra-trace gold(III)
Conjugate adsorbent
Detection and recovery
Urban mining waste
Reversibility

ABSTRACT

This study developed an efficient fine-tuning conjugate adsorbent for simultaneous gold (Au(III)) detection and recovery from urban mining waste. The adsorbent was prepared by indirect and dense immobilization of 6-((2-(2-hydroxy-1-naphthoyl)hydrazono)methyl) benzoic acid (HMBA) onto fine-tuned surface patterning of nanostructure inorganic silica. This adsorbent has the large surface area-to-volume ratios and uniformly shaped pores in nanostructures in its cage cavities. Therefore, the conjugate adsorbent permitted to fast and specific Au(III) ions capturing via a colorimetric naked-eye visualization based on the stable complexation $[Au(III)–HMBA]^{n+}$ mechanism. The small energy gap for the complex compared with the HMBA suggested the easily excitation of electrons according to the electron transfer or energy transferred mechanism, which results in the intense color of the stable complexation mechanism. The influence of several variables such as solution acidity, initial concentrations and the addition of diverse ions for Au(III) detection and recovery has also been considered and evaluated. The detection limit of the conjugate adsorbent at optimum conditions was 0.11 μg/L. The Au(III) sorption forms a monolayer on the interior pore surfaces of the conjugate adsorbent and showed high sorption capacity (203.42 mg/g). In addition, the sorption uptake on the adsorbent reaching equilibrium was rapid and adsorbent was also exhibited high Au(III) ion selectivity in ionic competition. Acidified thiourea was used in the elution of the Au(III) and conjugate adsorbent exhibited in terms of reproducibility and versatility over a number of analysis/regeneration cycles. Therefore, the present conjugate adsorbent offered a low-cost material for potential application of ultra-trace Au(III) detection and recovery from urban mining waste scraps.

1. Introduction

Gold has been widely used in many fields such as jewelry, many high-tech industries, and catalysts in various chemical processes, electrical and electronic industries and corrosion-resistant materials [1,2]. Moreover, gold (Au(III)) has been historically important and remain important as investment commodity due to its unique physical and chemical properties [3]. The increase in the industrial demand and its values and scarcity for Au(III), the need for Au(III) recycling to treat the waste aqueous solutions and recover the Au(III) economically has increased. However, the detection and recovery of Au(III) are not simple issue because of the low concentration of Au(III) in environmental, geological and metallurgical materials. In addition, the used different materials are lacked of insufficient selectivity and sensitivity to Au(III) ions [4–6]. Therefore, scientists are developing highly efficient and environment-friendly methods for Au(III) detection and recovery that the Au(III) can be selectively separated from coexisting diverse base metals in disproportionate amounts.

Many methods are reported to detect and quantify the Au(III) ions such as spectrophotometry, flame atomic absorption spectrometry (FAAS), graphite furnace (GFAAS) or electrothermal atomic absorption spectrometry (ETAAS), ICP–AES and inductively coupled plasma mass spectrometry (ICP–MS) [7,8]. These modern instrumental techniques are highly sensitive and selective. However, they are costly, complicated, time-consuming and not used for routine applications. Moreover, the direct Au(III) determination is to some extend a problem because of the interfering matrix components in real samples. Therefore, different functional group ligands trapped on a variety of solid matrices have been used for sensitive determination of trace Au(III) ions based on easy-to-use and cost effective adsorbents [9].

* Corresponding author. Tel.: +81 791 58 2642; fax: +81 791 58 0311.
E-mail addresses: rawual76@yahoo.com, awual.rabiul@jaea.go.jp (Md.R. Awual).

http://dx.doi.org/10.1016/j.snb.2014.02.055
0925-4005/

Several methods also have been used to separate and recover of Au(III) including solvent extraction, chemical precipitation, membrane separation, ion exchange and sorption [10–16]. Among these processes, solvent extraction is in extensive use because of its simplicity and effectiveness. However, various drawbacks such as high cost, time consuming, use of toxic solvents and large volumes of extractants and organic solvents are required and the release unacceptable chemicals waste makes the solvent extraction technique is unfavorable [17–19]. On the other hand, the sorption of a solute on a solid support has the advantage over solvent extraction in that no excessive slugged are produced and considered as environment friendly technology. Therefore, the sorption seems to be the most suitable method for the recovery of Au(III) based on cost effective and high efficiency [20,14,21–23]. In this connection, our focus is now towards developing various adsorbent materials for metal detection and recover from a variety of urban mining and environmental samples, as they are cheap, environmentally benign, reversible and reusable in several cycles.

Nanoscience and nanotechnology have gained considerable interest due to the needs and applications of nanomaterials in almost all areas of human endeavour [24–26]. The nanomaterials are the suitable candidate to be full-fill such a requirement with high sensitivity and selectivity in solid-liquid phase extraction, recovery and recognition of target ions [27]. The sensitivity and specific properties of nanoparticles materials resulting from the high surface-area-to-volume ratio make them suitable for a wide variety of applications. The ligands immobilized of these inorganic silica materials have drawn the considerable attention due to active functionality of the organic ligand with thermal and mechanical stabilities in such high surface area materials. The organic ligand to inorganic silica surfaces by covalent bonds followed co-condensation into the inorganic framework cross-links to accessible target metals ions capturing with high sensitivity. Therefore, different morphological shapes and functional materials are essential for simple, easy-to-use and selective trace metal ions capturing by adsorbents [28,29].

Recently, the mesoporous adsorbent for selective Au(III) sorption and recovery from electronic scraps has been reported [9]. However, this study focused in here the different ligand densely immobilized by indirect immobilization onto inorganic mesoporous silica for preparing fine-tuned conjugate adsorbent for highly selective to Au(III) ions even in the presence of large quantity competing ions. In this study, highly selective ligand of 6-((2-(2-hydroxy-1-naphthoyl) hydrazono)methyl)benzoic acid (HMBA) building block (indirect) immobilized onto inorganic silica materials was examined as a new class conjugate adsorbent for the simultaneous detection and recovery of Au(III) ions from urban mining waste scraps. The rapid synthesis approach using direct templating method of lyotropic liquid crystalline phase is believed to generate the bulk form of inorganic silica materials. The inorganic silica materials exhibited high ordered nanostructure, in which the pores were well arranged as nanocage structure with large pore volume and high surface area to use as an excellent carrier for the producing of ligand immobilized conjugate adsorbent for recognition and recovery of Au(III) ions. The conjugate adsorbent responses can be triggered by Au(III) ions and can transduce measurable signals at optimum pH conditions, enabling the sorption by stable complexation mechanism. This work also describes a simple and efficient conjugate adsorbent preparation with densely immobilizing ligand functionalization for Au(III) capturing systems. The experimental studies were carried out by batch approaches. The influence of various parameters such as solution acidity, color optimization, Au(III) sorption capacity, in the presence of competing ions and Au(III) recovery behavior was systematically investigated.

2. Materials and methods

2.1. Materials

All materials and chemicals were of analytical grade and used as purchased without further purification. Tetramethylorthosilicate (TMOS), the triblock copolymers of poly(ethylene oxide-b-propylene oxide-b-ethylene oxide) designated as F108 ($EO_{141}PO_{44}EO_{141}$) and 3-formylbenzoic acid were obtained from Sigma–Aldrich Company Ltd. USA. The standard Au(III) ions solutions, and metal salts for the source of metal ions were purchased from Wako Pure Chemicals, Osaka, Japan. For pH adjustments in naked-eye detection operation, buffer solutions of 3-morpholinopropane sulfonic acids (MOPS), 2-(cyclohexylamino) ethane sulfonic acid (CHES) and *N*-cyclohexyl-3-aminopropane sulfonic acids (CAPS) were procured from Dojindo Chemicals, Japan, and KCl, HCl, NaOH from Wako Pure Chemicals, Osaka, Japan. Ultrapure water prepared with a Millipore Elix Advant 3 was used throughout in this work.

2.2. Synthesis of HMBA ligand and inorganic mesoporous silica

The structure and preparation of the 6-((2-(2-hydroxy-1-naphthoyl)hydrazono)methyl) benzoic acid (HMBA) is shown in Scheme 1. The preparation method and characterization are reported elsewhere [30]. Here, the synthesis process was simplified for reader understanding. The HMBA was prepared by the reaction of 2-hydroxy-1-naphthohydrazide (one mole) and 3-formylbenzoic acid (one mole) in ethanol and small amount of acetic acid. The resultant mixture was then heated under reflux for 4 h and left to cool at room temperature. The solid formed upon cooling was collected by suction filtration. The separated product was recrystallized using dichloromethane/methanol 1/1 media. Then the product materials were dried at 50 °C for 24 h.

The F108 ($EO_{141}PO_{44}EO_{141}$, MW: 14,600) surfactant was used as scaffolds in preparation of inorganic silica materials. The preparation of inorganic silica materials procedure involved adding TMOS and triblock copolymers (F108) to obtain a homogenized sol-gel mixture based on the F108/TMOS mass ratio. An acidified aqueous solution was added to the mixture to achieve the desired liquid

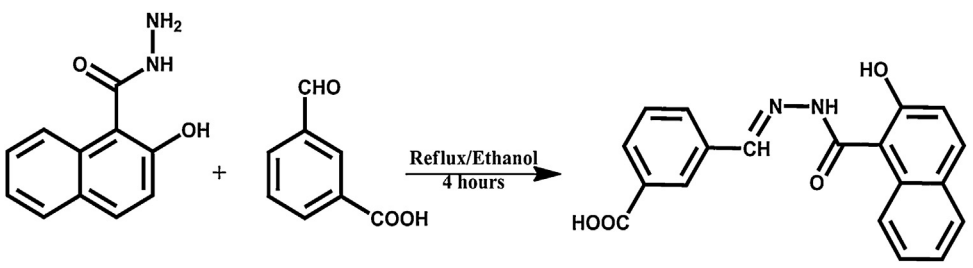

Scheme 1. Preparation steps and structure of 6-((2-(2-hydroxy-1-naphthoyl)hydrazono)methyl)benzoic acid (HMBA) ligand.

crystal phase and then to promote hydrolysis of the TMOS around the liquid crystal phase assembly of the triblock copolymer surfactants. The composition mass ratio of F108:TMOS:HCl/H_2O was 1.4:2:1 respectively. The detail preparation methods were reported elsewhere [28].

2.3. Preparation of fine-tuning conjugate adsorbent

The fine-tuning conjugate adsorbent was prepared by indirect immobilization approach. The mesoporous silica was polarble with the tuning facility by immobilization the dilauryl dimethyl ammonium bromide (DDAB) and then the HMBA was immobilized onto the tunable carriers. Here, 0.20 M ethanol solution of DDAB and 1.0 g of mesoporous silica monoliths were immobilized. Then the HMBA (60 mg) in ethanol solution was contacted with 1.0 g DDAB–masoporous inorganic silica. The immobilization procedure was performed under vacuum at 40 °C for 5 h stirring until HMBA ligand saturation was achieved. The ethanol was removed by a vacuum connected to a rotary evaporator at 45 °C and the resulting conjugate adsorbent was washed in warm water to check the stability and elution of HMBA from inorganic silica materials. Then the material was dried at 55 °C for 5 h and grinded to fine powder for Au(III) detection and recovery experiments. The HMBA immobilization amount (0.13 mmol/g) was determined by the following equation:

$$Q = \frac{(C_0 - C)V}{m} \quad (1)$$

where Q is the adsorbed amount (mmol/g), V is the solution volume (L), m is the mass of inorganic silica materials (g), C_0 and C are the initial concentration and supernatant concentration of the HMBA, respectively.

2.4. Au(III) ions detection

In detection, the conjugate adsorbent was immersed in a mixture of specific Au(III) ions concentrations (2.0 mg/L) and adjusted at appropriate pH of 1.01, 2.01, 3.0 (0.2 M of KCl with HCl), 5.20 (0.2 M $CH_3COOHCH_3COONa$ with HCl), 7.01 (MOPS with NaOH) and 9.50 (0.2 M 2-(cyclohexylamino) ethane sulfonic acid (CHES) with NaOH) in a specific amount of the conjugate adsorbent (10 mg) at constant volume (10 mL) with shaking in a temperature-controlled water bath with a mechanical shaker at 25 °C for 10 min at a constant agitation speed of 110 rpm to achieve good color separation. In addition, the blank solution was also prepared, following the same procedure for comparison of color formation. After color optimization, the solid materials were filtered using Whatman filter paper (25 mm; Shibata filter holder) and used for color assessment and absorbance measurements by solid-state UV–vis–NIR spectrophotometer for the qualitative and quantitative estimation of Au(III) ions. The adsorbent was ground into fine powder disks to achieve homogeneity in the reflectance spectra and absorbance. The detection limit (L_D) of Au(III) ions was determined from the linear part of the calibration plot according to the following equation [26]:

$$L_D = \frac{KS_b}{m} \quad (2)$$

where K value is 3, S_b is the standard deviation for the blank and m the slope of the calibration graph in the linear range, respectively.

2.5. Au(III) sorption, recovery and reversibility of conjugate adsorbent

In sorption systems, the conjugate adsorbent was also immersed in Au(III) ions concentrations and adjusted at specific pH values by adding of HCl or NaOH in 20 mL solutions for 1 h at room temperature and amount of adsorbent was also used of 10 mg. Then the adsorbent was separated by filtration system and Au(III) concentrations in before and after sorption operations were analyzed by ICP–AES. The batch sorption experiments were performed at room temperature (25 °C). The amount of adsorbed Au(III) was calculated according to the following equations:

$$\text{Mass balance } q_e = \frac{(C_0 - C_f)V}{M} \text{ (mg/g)} \quad (3)$$

and

$$\text{Au(III)sorption efficiency } Re = \frac{(C_0 - C_f)}{C_0} \times 100 \ (\%) \quad (4)$$

where V is the volume of the aqueous solution (L), and M is the weight of the conjugate adsorbent (g), C_0 and C_f are the initial and final Au(III) ions concentrations in solutions, respectively.

In case of recovery system, first 20 mL of 2.0 mM Au(III) ion solution was adsorbed by the 20 mg adsorbent and then recovery experiments were carried out using various concentrations of H_2SO_4, HCl, and HCl–thiourea solutions. The adsorbed Au(III) metal ions onto conjugate adsorbent was washed with deionized water several times and transferred into 50 mL beaker. To this 5 mL of the stripping agent was added, and then the solutions were stirred for 15 min. The concentration of Au(III) ion released from the adsorbent into aqueous phase was analyzed by ICP–AES. Then the conjugate adsorbent was reused several cycles to investigate the reusability. All experiments in this study were duplicated to assure the consistency and reproducibility of the results.

2.6. Instruments and analyses

The N_2 adsorption-desorption isotherms were measured using BELSORP MINI-II analyzer (JP. BEL Co. Ltd.) at 77 K. The pore size distribution was measured from the adsorption isotherms plot by using nonlocal density functional theory (NLDFT). The inorganic silica material was pre-treated at 100 °C for 3 h under vacuum until the pressure was equilibrated to 10^{-3} Torr before the N_2 isothermal analysis. The specific surface area (S_{BET}) was measured by using multi-point adsorption data from linear segment of the N_2 adsorption isotherms using Brunauer–Emmett–Teller (BET) theory. The NMR spectra was obtained on a Varian NMR System 400 MHz Spectrometer. Transmission electron microscopy (TEM) was obtained by using a JEOL (JEM-2010) and operated at the accelerating voltage of the electron beam 200 kV. The TEM samples were prepared by dispersing the powder particles in ethanol solution using an ultrasonic bath and then dropped on copper grids. The absorbance spectrum was measured by UV–vis–NIR spectrophotometer (Shimadzu, 3700). The metals ion concentrations were measured by ICP–AES (SII NanoTechnology Inc.). The ICP–AES instrument was calibrated using five standard solutions containing 0, 0.5, 1.0, 1.5 and 2.0 mg/L (for each element), and the correlation coefficient of the calibration curve was higher than 0.9999. In addition, sample solutions having complicated matrices were not used and no significant interference of matrices was observed.

Restricted closed-shell DFT-B3LYP calculation formula [31,32] and fully optimized calculation strategy were employed to study and the stability of Au(III) complex formed with HMBA. Geometries were predicted using 6-31+G(d,p) basis set for the ligand, and LANL2DZ relativistic effective core potential (RECP) basis set for Au atom [32,33].

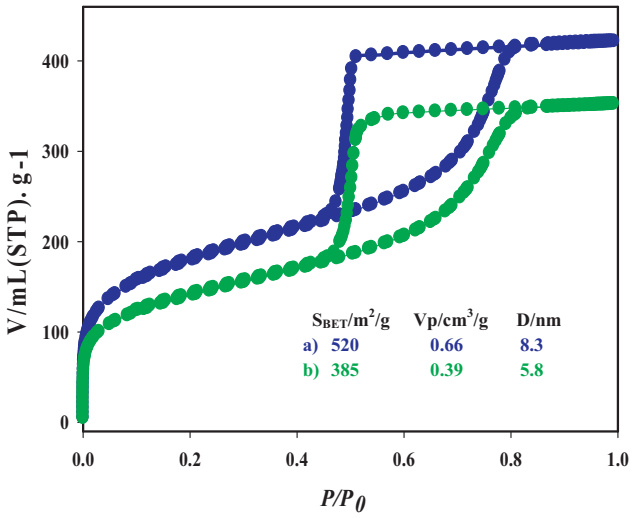

Fig. 1. N_2 adsorption/desorption isotherms at 77 K (a) high ordered inorganic silica materials synthesized by using direct templating method and (b) fine-tuning conjugate adsorbent with difference of high surface areas and large pore sizes and volumes.

3. Results and discussion

3.1. Inorganic mesoporous silica and fine-tuning conjugate adsorbent

The N_2 isotherms show the typical type IV adsorption behaviors with a broad hysteresis loop of H_2 type adsorption branches were significantly shifted toward lower relative pressure (P/P_0) (Fig. 1). The N_2 adsorption–desorption measurements indicated that the tuning silica materials possess good mesopore structure ordering and a relatively narrow pore size distribution. The silica materials showed the appreciable surface area (S_{BET}), mesopore volume (V_p), and tunable pore diameters. The framework porosity also indicated that the porosity within the uniform channels implied the presence of framework and textural porosity [28,29]. Large pore volume, pore diameter and high surface area of the inorganic silica materials indicated that the samples have nanoporous structure in its case cavities. In such preparation of conjugate adsorbent without additive coupling agents clarify the low operating cost. Such material has great advantages for fabrication of ligand immobilized conjugate adsorbent to detect and separation of ultra-trace Au(III) ions from urban mining waste.

The scanning electron microscopy images of as-synthesized samples are typical of the silica materials and show large particle morphologies (Fig. 2(A and B)). A higher magnification SEM image indicated the presence of macropores of various sizes ranging from 1 to 10 μm. In addition, the particles were almost perfectly spherical in shape and size. The mesoporous silica exhibited high ordered mesoporous structure, in which the pores were well arranged as mesocage structure as judged from Fig. 2(C). Higher magnification TEM image (Fig. 2(D)) indicated the highly ordered porous structure of mesocage silica with average pore size of about 7.5 nm, which indicate the interaction between the HMBA and tunable inorganic silica into the rigid condensed pore surfaces with retention of the ordered structures, leading to high flux and Au(III) ion transport during detection and sorption processes. In addition, the TEM image exhibited well-organized parallel channels and clarified a hexagonally ordered array in the direction parallel to the pore which clarified the prepared material has a typical hexagonal [30]. After successful HMBA immobilization onto tunable mesoporous silica, the appreciable pores were also ordered as depicted in Fig. 2(E and F).

The fine-tuning conjugate adsorbent was fabricated by indirect immobilization approach. After immobilization of HMBA, a decrease in the surface area (S_{BET}) and average pore diameter of conjugate adsorbent provided further the presence of HMBA ligand on the surface partially blocks the adsorption of nitrogen molecules as judged from Fig. 1(b) [26]. The materials characterization also confirmed that the ability to achieve flexibility in the specific activity of the electron acceptor or donor strength of the chemically responsive HMBA ligand molecule may lead to easy generation and transduction of visual color signal in the naked-eye visualized detection and sorption of ultra-trace Au(III) ions by the stable complexation mechanism.

3.2. Ultra-trace Au(III) detection

The pH is a key control factor in the selective detection in the proposed Au(III) detection system using adsorbent. In optimum pH conditions for the acceptor–donor combinations between

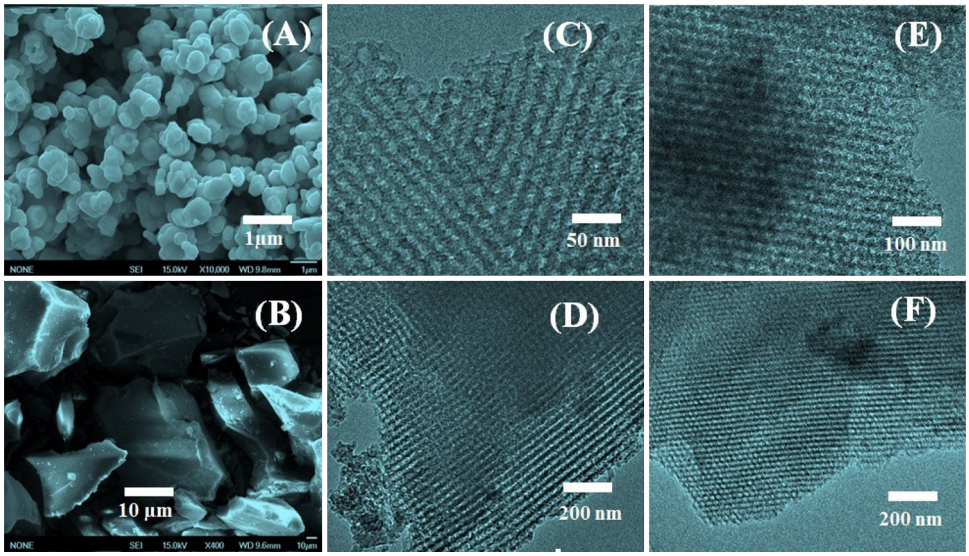

Fig. 2. SEM images of the inorganic silica materials prepared by instant direct-templating method (A and B); TEM images representative of ordered nanostructures along with uniformly arranged pores in all direction (C and D) and also TEM images of the fine-tuning conjugate adsorbent (E and F).

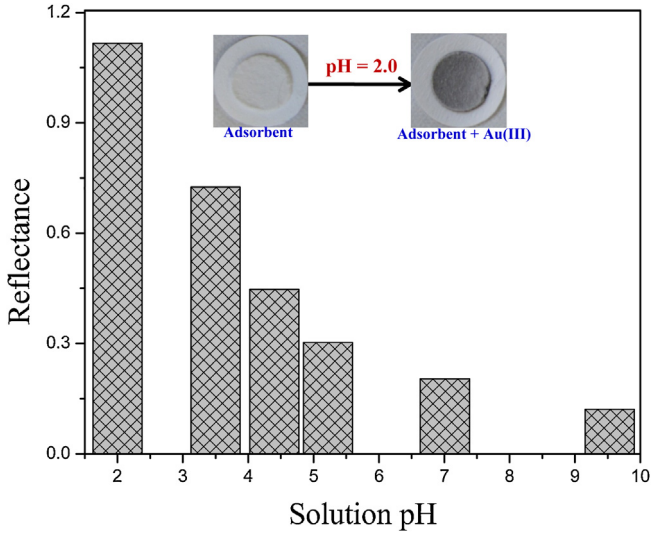

Fig. 3. Effect of pH for ultra-trace Au(III) detection by conjugate adsorbent. The equilibrated individually at different pH conditions with 2.0 mg/L of Au(III) ions at 25 °C in 10 mL volume for 10 min. The standard deviation was >2.5% for the analytical data of duplicate analyses.

Au(III) and HMBA ligand on the conjugate adsorbent surface, the reflectance spectra of the Au(III)–adsorbent complexes on pore surfaces were evaluated over a wide range of pH (Fig. 3). The absorbance spectra of $[Au(III)–HMBA]^{n+}$ complex at $\lambda = 550$ nm was carefully recorded. The absorbance intensity reached the maximum when pH was 2.0. The signalling of Au(III) ions by the conjugate adsorbent is mainly dependent on the stability to form the stable complex of Au(III)–HMBA binding at the specific pH conditions [29]. Such stable reactions facilitate the formation of $[Au(III)–HMBA]^{n+}$ complexes with a remarkable response in detection and sorption systems. Moreover, pH 2.0 was chosen as optimum experimental condition in accordance with sensitivity and selectivity.

The color optimization by charge transfer (intense π–π transition) reflection band of the $[Au(III)–HMBA]^{n+}$ complexes depended on the HMBA-binding affinity. The reflectance spectra enhancement and color optimization of the conjugate adsorbent was monitored during the formation of $[Au(III)–HMBA]^{n+}$ complexes with increasing the Au(III) ions concentration as shown in Fig. 4(A). The reflectance spectra was observed at λ_{max} of 550 nm as a result of complexation and the signaling detect of Au(III) ions with the HMBA ligand. The color change provided a simple procedure for the sensitive and selective detection of Au(III) ions without the need for highly sophisticated instruments. In such a sensitive Au(III) detection at ultra-trace concentrations by using the naked-eye observation indicated the high performance and reliability of the conjugate adsorbent.

The calibration curve was prepared by analyzing the standard solutions with different Au(III) ions concentrations at optimum pH as shown in Fig. 4(B). The calibration plots of the conjugate adsorbent show a linear correlation at low concentration of Au(III) ions. The linear correlation at low concentration range clarified that the Au(III) could be detected with high sensitivity in different concentrations level. In addition, a nonlinear correlation at the inflection point was evident to the highest concentration of Au(III) ions, indicating that sensitive detection of low concentrations of Au(III) ions. The detection limit value indicated that the detection system could detect Au(III) ions at concentrations down to 0.11 μg/L, even in presence of the several matrices (calibration curve with dotted lines). The error bar denotes a relative standard deviation of approximately 2% for the analytical data of five replicate analyses. A linear correlation in the range from 0.025 to 0.508 μM was observed and higher concentration over 0.508 μM, the dependence was nonlinear due to saturation effects.

The specific ion selectivity of the conjugate adsorbent is crucial due to co-existing of interfering ions and species [9,26,29]. The Au(III) ion selectivity was investigated at optimum detection conditions. In this investigation, the competing ions (Cu^{2+}, Mg^{2+}, Hg^{2+}, Pd^{2}+, Ca^{2+}, Pt^{2+}, Ru^{3+}, Ni^{2+}, Al^{3+}, Co^{2+}, Fe^{3+}, Cr^{3+} and Bi^{3+}) concentration was 10-folds higher than the Au(III) ion concentration. These ions were considered to be interfered if it resulted in a ±5% variation of the absorbance. Fig. 5 shows the color profiles and absorbance spectra and differences of the blank sample and after the addition of competing ions signals responses in accordance with reflectance spectra. The data clarified that the divers competing ions did not show any considerable spectral change compared with blank sample except Au(III) ions. However, with the addition of high concentration (50 folds) of these actively interfered ions to the Au(III) ions detection system, a high disturbance (±15%) in the quantitative Au(III) ions recognition was evident. The results

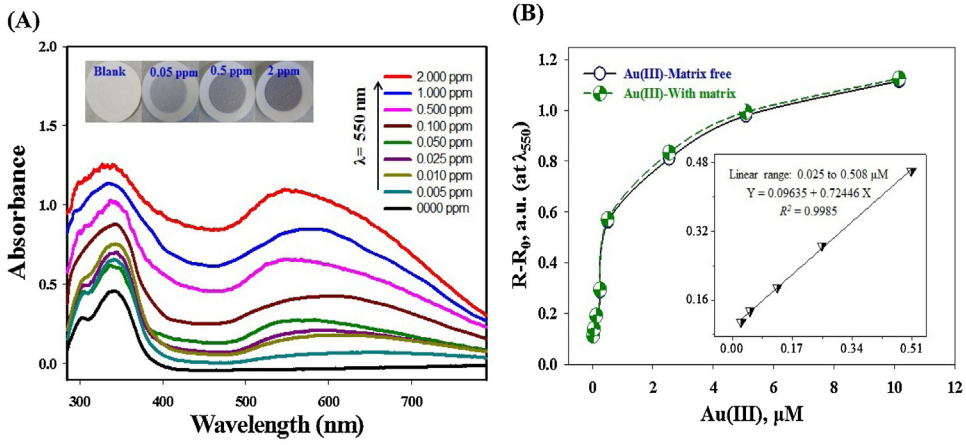

Fig. 4. (A) Color optimization at different initial Au(III) concentrations corresponds to the reflectance spectral and (B) representative calibration profile with spectral absorbance measured at 550 nm with Au(III) ion concentrations. The inlets in graphs (B) show the low-limit signal responses for Au(III) ions with a linear fit in the linear concentration range. The R and R_0 are the absorbance signal responses of the adsorbent after and before addition of Au(III) ion. The dotted line represents the calibration plot of the Au(III) ions in presence of active interfering species under the same determination conditions. The error bars denote a relative standard deviation of ≥2% range for the analytical data of 5 replicated analyses. (For interpretation of the references to color in this figure legend, the reader is referred to the web version of the article.)

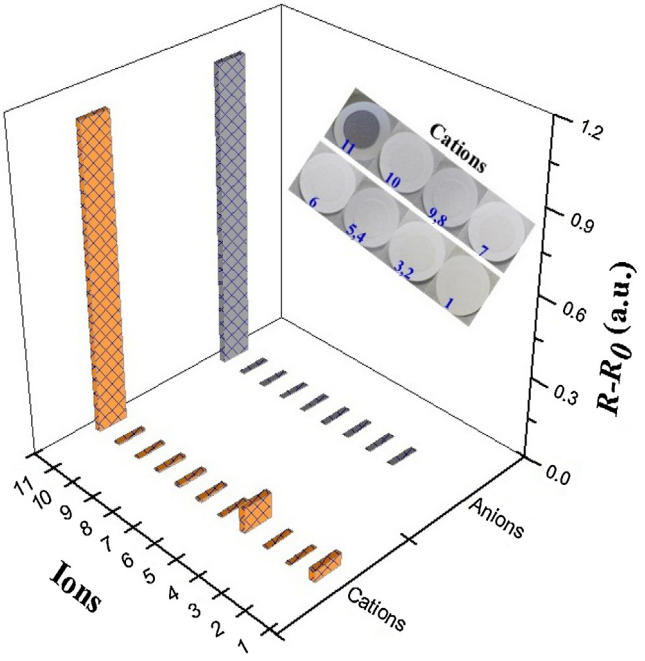

Fig. 5. Color transition ion selectivity profiles of the conjugate adsorbent after adding different metal ions at optimal conditions. The interfering cations (20.0 mg/L) listed in order (1 to 11): (1) Cu^{2+}, Co^{2+}, (2) Mg^{2+}, Ca^{2+}, (3), Hg^{2+}, (4) Pd^{2+}, (5) Pt^{2+}, Ru^{3+}, (6) Ni^{2+}, (7) Al^{3+}, (8) Ag^{+}, (9) Fe^{3+}, (10) Bi^{3+}, Cr^{3+}, (11) Blank and (12) 2.0 ppm Au^{3+}. The interfering (500 mg/L) anions listed in order (3–10): (3) chloride, (4) nitrate, (5) sulfate, (6) phosphate, (7) bicarbonate, (8) carbonate, (9) citrate and (10) perchlorate. (For interpretation of the references to color in this figure legend, the reader is referred to the web version of the article.)

indicated that conjugate adsorbent has selectivity to Au(III) ions due to strong tendency to form a stable complexation with HMBA ligand.

3.3. Reaction mechanism

From the theoritical calculation, the bonding mechanism was illustrated at pH 2.0 for the stable complexation mechanism. The DFT calculation plays a unique role in structure analysis of metal complexes. Moreover, it gives first insight about the chemical reactivity of molecular species. Optimization of HMBA showed that it has a planner shape as shown in Fig. 6(a). The atomic charge distribution on HMBA reflected that the imino nitrogen (–N=C) was more negative than the adjacent amide nitrogen (–HN–C=O), therefore, HMBA was expected to form coordination bond through the imino group. Au(III) forms square planner complexes [34]. Optimization indicated a monodentate coordination of HMBA though the imino nitrogen. In addition, Au(III) completed the square planner coordination with three anions (Cl^- in this case) (Fig. 6(b)).

The chemical reactivity of the formed complex was evaluated from the calculated highest occupied molecular orbital (HOMO) and the lowest unoccupied molecular orbital (LUMO). Specifically, global chemical reactivity descriptors (energy gap, chemical hardness, electronic chemical potential and electrophilicity) were calculated [35–37]. The physical meanings of these descriptors are defined as follows: Chemical hardness (η) in a molecule refers to the resistance to change in the electron distribution or charge transfer. The electronic chemical potential (μ) is a measure of electronegativity of the molecule. The electrophilicity index (ω), measures the capacity of a species to accept electrons. Table 1 summarizes the computed chemical descriptors for HMBA and [Au(HMBA)·Cl_3] structures. The electronic chemical potential (μ) was associated with the stability and reactivity of a chemical system. The greater μ, the less stable or more reactive is the molecule. Therefore, [Au(HMBA)·Cl_3] is more stable than HMBA. The calculated energy gap ΔE for the HMBA ligand and it Au(III) complexes were 4.18 eV and 2.06 eV, respectively. The small energy gap for the complex compared with the ligand suggested the easily excitation of electrons according to the electron transfer (eT) or energy transfer (ET) mechanism, which results in the intense color of the complex.

Table 1
The calculated HOMO, LUMO, energy gap (ΔE), electronic chemical potential (μ), chemical hardness (η), and electrophilicity (ω) of the HMBA and [Au(HMBA)·Cl_2] complex, all energy values are in eV unit.

Complex	HOMO	LUMO	ΔE	μ	η	ω
HMBA	−6.09	−1.91	4.18	−4.00	2.09	3.83
[Au(HMBA)·Cl_2]	−6.78	−4.72	2.06	−5.75	1.03	16.05

3.4. Au(III) sorption, recovery and regeneration studies

The solution pH is also a significant parameter for sorption of target metal ions due to the effect of structural properties of the adsorbent and metals ions based on the pH values. Therefore, pH of Au(III) solution plays a key role during the sorption process by the conjugate adsorbent. The effect of solution acidity of the medium on Au(III) uptake was determined and the results are presented in Fig. 7(A). The variation in the sorption of Au(III) was evaluated within the pH range of 2.0–7.0 by the conjugate adsorbent. The optimum pH for the uptake of Au(III) was an acidic condition of pH 2.0 as judged from Fig. 7(A). With increasing pH, the Au(III) sorption is decreased by different adsorbents materials [19]. However, ligand embedded conjugate adsorbent has a specific sorption ability at the specific pH region for target metal ions [25,26].

In order to know the suitable contact time for maximum sorption efficiency, the equilibrium contact was also evaluated. Fig. 7(B) shows the effect of contact time for maximum Au(III) sorption by the conjugate adsorbent. The data clarified that the increasing in contact-time increased the sorption efficiency. The maximum sorption efficiency was achieved within 1 h at room temperature. However, solvent extraction and biosorption are bit slow kinetics than the ion exchange and complexation sorption mechanisms [38,39].

The Au(III) ions distribution between the conjugate adsorbent and the Au(III) solution under equilibrium conditions is importance factor in the evaluation of maximum sorption capacity by proposed conjugate adsorbent. In addition, an equilibrium sorption is one of the important physicochemical aspects to the evaluation of the sorption process as a unit operation. The equilibrium sorption of the conjugate adsorbent for Au(III) ions was investigated through sorption isotherms whose parameters include q_e (mg/g), the quantity of Au(III) adsorbed per unit mass of the conjugate adsorbent, and C_e (mg/L), the equilibrium Au(III) ions concentration in the solution. The sorption studies were conducted by varying the initial Au(III) ions concentration while the conjugate adsorbent dose in each sample was kept identical. Based on Langmuir sorption theory, the sorption takes place at specific homogeneous sites on the conjugate adsorbent. In this case, when a site is occupied by a solute, no further sorption can take place at that site. Therefore, the Langmuir sorption isotherm based on the assumption of all sorption sites are energetically same and sorption occurs on a structurally homogeneous adsorbent. Then the Langmuir equation has been successfully applied to this sorption operation as follows:

$$\frac{C_e}{q_e} = \frac{1}{(KLq_m)} + \left(\frac{1}{q_m}\right) C_e \,(\text{linear form}) \quad (5)$$

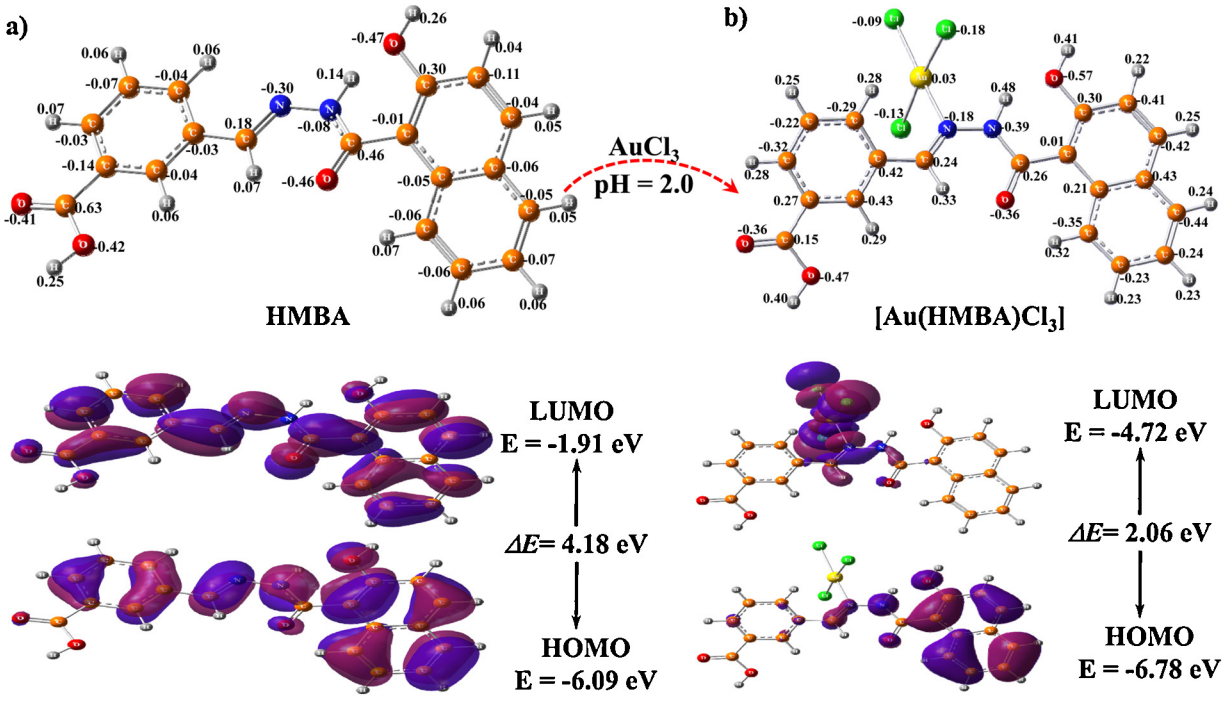

Fig. 6. Optimized structures of (a) HMBA ligand and (b) [Au(HMBA)Cl_3] complex with their calculated HOMO–LUMO orbitals occupations and the calculated energy gap.

where q_m is the maximum sorption capacity, K_L is the Langmuir coefficient (L/mg), q_e is the amount of adsorbed Au(III) ions on conjugate adsorbent at equilibrium (mg/g) and C_e is the equilibrium liquid concentration (mg/L). The sorption isotherms (q_e versus C_e) showed that the sorption capacity, which is the mass (mg) of total Au(III) ions adsorbed per unit mass of adsorbent, increased with increasing equilibrium Au(III) ions concentration and eventually attained a constant value (Fig. 8). The q_m and K_L are the Langmuir constants which are related to the sorption capacity and energy of sorption, respectively, and can be calculated from the intercept and slope of the linear plot, with C_e/q_e versus C_e as shown in Fig. 8 (inset). The correlation coefficients value ($R^2 = 0.9916$) confirm that the Langmuir sorption equation can be considered an accurate model of the sorption behavior of the conjugate adsorbent. The essential characteristics of the Langmuir isotherm can be expressed in terms of a dimensionless constant separation factor or equilibrium parameter, R; which is defined by the following equation:

$$R = \frac{1}{1 + K_L C_0} \quad (6)$$

where K_L is the Langmuir constant and C_0 is the initial concentration of Au(III). The R values in this study ranged below the unit, indicating the favorable sorption process on conjugate adsorbent at the concentrations studied. The good applicability of the Langmuir isotherms clarified that monolayer sorption and homogeneous distribution of active groups on the surface was evident. The maximum sorption capacity corresponding to complete monolayer coverage showed a mass capacity of 203.42 mg/g and the sorption coefficient K_L, which is related to the apparent energy of sorption, was calculated to be 2.17 L/mg.

The sorption capacity compared with literature values [9,19,20,14,21,22,40,41] listed in Table 2. The conjugate adsorbent was found to be comparable and competitive with other forms of adsorbent materials. It was initially assumed that the higher maximum sorption capacity obtained for Au(III) by the conjugate adsorbent due to the spherical and fine-tuning nanosized cavities with large surface area of the adsorbent would allow an increased equilibrium sorption capacity.

The presence of co-existing metal ions affected the sorption affinity of Au(III) and it is the most important issue to investigate

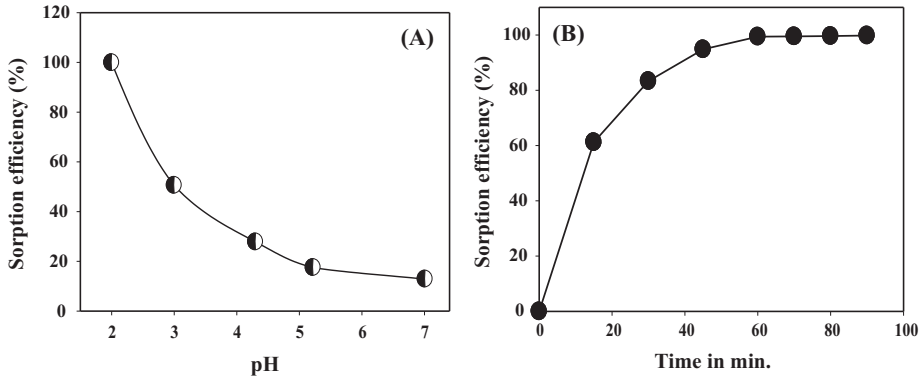

Fig. 7. (A) High sorption of Au(III) ions by the conjugate adsorbent under different pH solutions; (B) equilibrium sorption efficiency in relation with suitable contact time (5.0 mg/L Au(III) ions in 20 mL). The RSD value was ~3.0%.

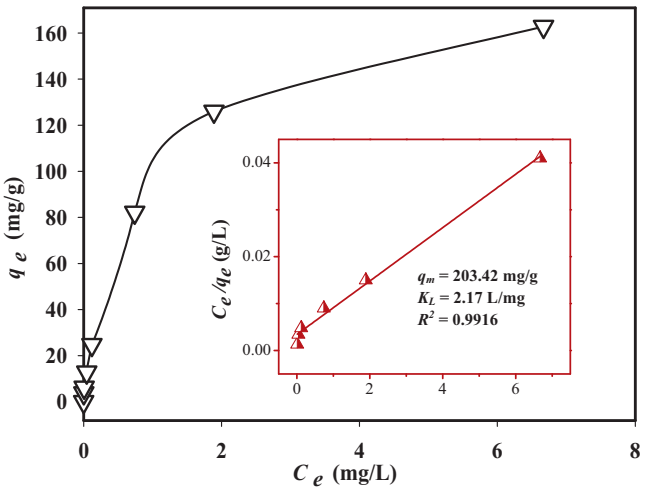

Fig. 8. Langmuir sorption isotherms of Au(III) ions and the linear form of the Langmuir plot (initial Au(III) ion concentration range 1.02–75.16 mg/L; solution pH 2.0; dose 8 mg; solution volume 30 mL and contact time 3 h).

Table 2
Comparison of sorption capacities towards Au(III) by using various adsorbent materials.

Used adsorbents	Capacity (mg/g)	Ref.
Lysine modified crosslinked chitosan resin	70.34	[16]
Glycine modified crosslinked chitosan resin	169.39	[17]
Thiol cotton fiber	54–68	[18]
Mesoporous adsorbents	200	[19]
XAD-7	98.48	[20]
Ion exchange resin	449.09	[40]
Wet carbon adsorbent	106.25	[41]
Mesoporous adsorbent	177.94	[9a]
Conjugate adsorbent	183.42	[9b]
Fine-tuning conjugate adsorbent	203.42	This study

the sorption selectivity of the conjugate adsorbent to Au(III) ions. A series of representative binary metal ion and multi-mixture ions systems were chosen to investigate the sorption selectivity of conjugate adsorbent for Au(III) and the results were shown in Fig. 9(A) (data are only from multi–mixture ions). The data obviously presented that Au(III) was readily adsorbed by the conjugate adsorbent from the systems of Au(III)–Fe(III), Au(III)–Cu(II), Au(III)–Ni(II), Au(III)–Zn(II), Au(III)–Pt(II), Au(III)–Ru(III), Au(III)–Ag(I) and Au(III)–Fe(III)–Cu(II)–Ni(II)–Zn(II)–Pt(II)–Ru(III)–Ag(I), respectively, and sorption percentage of the conjugate adsorbent for Au(III) was more than 97%, indicating that the conjugate adsorbent exhibited good sorption selectivity for Au(III). This high selectivity was due to high affinity of Au(III) ion to nitrogen donor atoms in HMBA ligand embedded conjugate adsorbent. Therefore, the conjugate adsorbent signifies its potential applicability for recovery of Au(III) from urban mining waste of industrial electronic scrap.

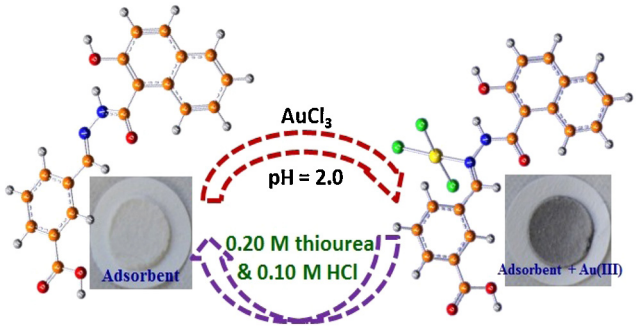

Scheme 2. Complexation mechanism of Au(III) with HMBA in optical detection and sorption processes and also the elution/recovery of Au(III) with 0.20 M thiourea–0.10 M HCl.

The Au(III) ions recovery depends on the Au(III) elution efficiency of the adsorbed Au(III) ions onto the conjugate adsorbent. Therefore, elution efficiency was evaluated in this study based on the ratio of the Au(III) desorbed from the conjugate adsorbent to the Au(III) adsorbed onto the adsorbent. Then the adsorbent was saturated with Au(III) ion in presence of competing ions and evaluate the exact eluent for complete recovery of Au(III) from the conjugate adsorbent. In treated with 1.0 M HCl, very low concentration of undesired metals ions were desorbed while these were adsorbed during Au(III) sorption operation. The experimental data confirmed that 0.20 M thiourea–0.10 M HCl was suitable to recover the Au(III) ions from the conjugate adsorbent. In elution operations, the conjugate adsorbent was simultaneously regenerated into the initial form without nanostructural damage of the conjugate adsorbent. The expected Au(III) complexation binding and recovery of Au(III) is shown in Scheme 2. The reusability was also measured of each sorption–elution cycles for nine cycles, and the sorption efficiency in each cycle was measured. The data were clarified that the Au(III) sorption efficiency slightly decreased after nine cycles (Fig. 9(B))

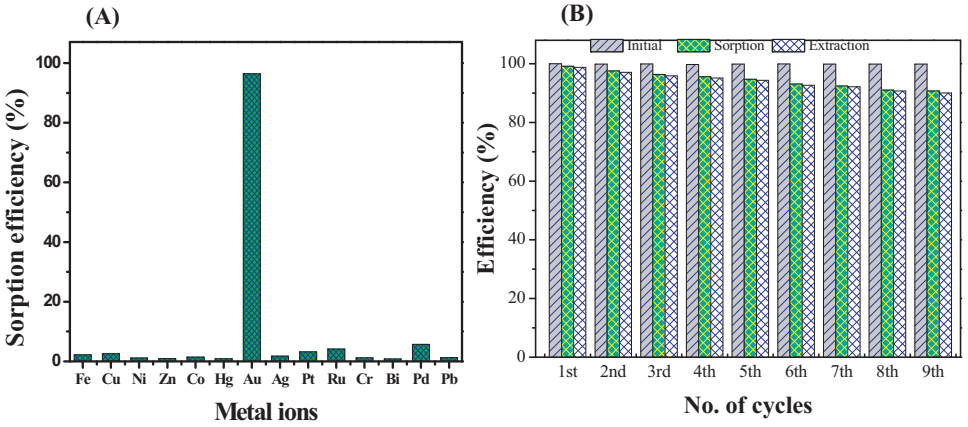

Fig. 9. (A) The Au(III) sorption in presence of competitive multi-metal ions from the solutions by the fine-tuning conjugate adsorbent. For sorption of 2 mg/L Au(III) from a mixture of metal ions including (i) 5.0 mg/L of Pt^{2+}, Ru^{3+}, Pd^{2+} and Ag^{+} each, and (ii) 40 mg/L of Fe^{3+}, Cu^{2+}, Ni^{2+}, Zn^{2+}, Co^{2+}, Hg^{2+}, Cr^{3+}, Bi^{3+} and Pb^{2+} each, respectively; (B) ICP–AES analysis of Au(III) ions after completing sorption and extraction within nine cycles. The RSD values were ~4.0%.

indicating the many cycles uses for Au(III) recovery operations by the conjugate adsorbent.

4. Conclusions

The Au(III) capturing by fine-tuning conjugate adsorbent in nanoscale level led to new frontiers in nanoscience and nanotechnology. The adsorbent was successfully prepared with 6-((2-(2-hydroxy-1-naphthoyl)hydrazono)methyl)benzoic acid (HMBA) immobilized onto polarable inorganic silica materials. The conjugate adsorbent exhibited interesting high level ion selectivity and permits accurate with specific detection and recovery of ultra-trace Au(III) in different concentrations via a colorimetric signal visible to the naked eye with UV–vis reflectance spectroscopy measurement in rapid response times. The equilibrium sorption data were well fitted with Langmuir isotherm model and confirmed the monolayer Au(III) sorption onto the conjugate adsorbent surface. The reducibility and reversibility of the conjugate adsorbent remain a unique and interesting challenge, however, the nanostructured conjugate adsorbent was captured the Au(III) even after several regeneration cycles of the elution/extraction process. The study also clarified the advantages of nanoscale pore geometry and shape, and particle morphology of the inorganic silica materials, in the design of conjugate adsorbent for efficient and accurate Au(III) capturing functionality in terms of sensitivity and selectivity. Such promising results are recommended to apply in large-scale for ultra-trace Au(III) detection and recovery systems from urban mining waste.

Acknowledgments

This research was partially supported by the Grant-in-Aid for Research Activity Start-up (24860070) from the Japan Society for the Promotion of Science. The author also wishes to thank the anonymous reviewers and editor for their helpful suggestions and enlightening comments.

References

[1] C.R.M. Rao, G.S. Reddi, Platinum group metals (PGM), occurrence, use and recent trends in their determination, Trends in Analytical Chemistry 19 (2000) 565–586.
[2] J. Cui, L. Zhange, Metallurgical recovery of metals from electronic waste: a review, Journal of Hazardous Materials 158 (2008) 228–256.
[3] H.Y. Kang, J.M. Schoenung, Electronic waste recycling: a review of U.S. infrastructure and technology options, Resource Conservation and Recycling 45 (2005) 368–400.
[4] I.D.L. Calle, N. Cabaleiro, M. Costas, F. Pena, S. Gil, I. Lavilla, C. Bendicho, Ultrasound-assisted extraction of gold and silver from environmental samples using different extractants followed by electrothermal-atomic absorption spectrometry, Microchemical Journal 97 (2011) 93–100.
[5] P. Liang, E. Zhao, Q. Ding, D. Du, Multi-walled carbon nanotubes microcolumn preconcentration and determination of gold in geological and water samples by flame atomic absorption spectrometry, Spectrochimica Acta B 63 (2008) 714–717.
[6] J. Hassan, M. Shamsipur, M.H. Karbasi, Single granular activated carbon microextraction and graphite furnace atomic absorption spectrometry determination for trace amount of gold in aqueous and geological samples, Microchemical Journal 99 (2011) 93–96.
[7] A.S. Amin, Utility of solid phase extraction for spectrophotometric determination of gold in water, jewel and ore samples, Spectrochimica Acta Part A 77 (2010) 1054–1058.
[8] E.A. Moawed, M.F. El-Shahat, Synthesis, characterization of low density polyhydroxy polyurethane foam and its application for separation and determination of gold in water and ores samples, Analytica Chimica Acta 788 (2013) 200–207.
[9] (a) M.R. Awual, M.A. Khaleque, M. Ferdows, A.M.S. Chowdhury, T. Yaita, Rapid recognition and recovery of gold(III) with functional ligand immobilized novel mesoporous adsorbent, Microchemical Journal 110 (2013) 591–598;
(b) M.R. Awual, Investigation of potential conjugate adsorbent for efficient ultra-trace gold(III) detection and recovery, Journal of Industrial and Engineering Chemistry (2013), http://dx.doi.org/10.1016/j.jiec.2013.12.040.
[10] H. Koyanaka, K. Takeuchi, C.K. Loong, Gold recovery from parts-per-trillion-level aqueous solutions by a nanostructured Mn_2O_3 adsorbent, Separation and Purification Technology 43 (2005) 9–15.
[11] Y.Z. Zhao, The enrichment and separation of race gold, Pt and Pd from the ores based on co-precipitation, Gold 27 (2006) 42–44.
[12] J. Sanchez-Martin, J. Beltran-Heredia, P. Gibello-Perez, Adsorbent biopolymers from tannin extracts for water treatment, Chemical Engineering Journal 168 (2011) 1241–1247.
[13] R. Al-Merey, Z. Hariri, J.A. Hilal, Selective separation of gold from iron ore samples using ion exchange resin, Microchemical Journal 75 (2003) 169–177.
[14] M. Yu, D. Sun, W. Tian, G. Wang, W. Shen, N. Xu, Systematic studies on adsorption of trace elements Pt, Pd, Au, Se, Te, As, Hg, Sb on thiol cotton fiber, Analytica Chimica Acta 456 (2002) 147–155.
[15] M. Baghalha, Leaching of an oxide gold ore with chloride/hypochlorite solutions, International Journal of Mineral Processing 82 (2007) 178–186.
[16] M. Hidalgo, A. Uheida, V. Salvado, C. Fontas, Study of the sorption and separation abilities of commercial solid-phase extraction (SPE) cartridge Oasis MAX towards Au(III), Pd(II), Pt(IV) and Rh(III), Solvent Extraction & Ion Exchange 24 (2006) 931–942.
[17] S. Akita, L. Yang, H. Takeuchi, Solvent extraction of gold(III) from hydrochloric acid media by nonionic surfactants, Hydrometallurgy 43 (1996) 37–46.
[18] A.G. Kilic, S. Malci, O. Celikbicak, N. Sahiner, B. Salih, Gold recovery onto poly(acrylamide-allylthiourea) hydrogels synthesized by treating with gamma radiation, Analytica Chimica Acta 547 (2005) 18–25.
[19] K. Fujiwara, A. Ramesh, T. Maki, H. Hasegawa, K. Ueda, Adsorption of platinum(IV), palladium (II) and gold (III) from aqueous solutions on to l-lysine modified crosslinked chiotosan resin, Journal of Hazardous Materials 146 (2007) 39–50.
[20] A. Ramesh, H. Hasegawa, W. Sugimoto, T. Maki, K. Ueda, Adsorption of gold(III), platinum(IV) and palladium(II) onto glycine modified crosslinked chitosan resin, Bioresource Technology 99 (2008) 3801–3809.
[21] K.F. Lam, C.M. Fong, K.L. Yeung, G. Mckay, Selective adsorption of gold from complex mixtures using mesoporous adsorbents, Chemical Engineering Journal 145 (2008) 185–195.
[22] M. Laatikainen, E. Paatero, Gold recovery from chloride solutions with XAD-7: Competitive adsorption of Fe(III) and Te(IV), Hydrometallurgy 79 (2005) 154–171.
[23] S.Y. Bratskaya, A.S. Volk, V.V. Ivanov, A.Y. Ustinov, N.N. Barinov, V.A. Avramenko, A new approach to precious metals recovery from brown coals: Correlation of recovery efficacy with the mechanism of metal–humic interactions, Geochimica Cosmochimica Acta 73 (2009) 3301–3310.
[24] F. Hoffmann, M. Cornelius, J. Morell, M. Froba, Silica-based mesoporous organic–inorganic hybrid materials, Angewandte Chemie International Edition 45 (2006) 3216–3251.
[25] M.R. Awual, M. Ismael, T. Yaita, S.A. El-Safty, H. Shiwaku, Y. Okamoto, S. Suzuki, Trace copper(II) ions detection and removal from water using novel ligand modified composite adsorbent, Chemical Engineering Journal 222 (2013) 67–76.
[26] (a) M.R. Awual, T. Kobayashi, Y. Miyazaki, R. Motokawa, H. Shiwaku, S. Suzuki, Y. Okamoto, T. Yaita, Evaluation of lanthanide sorption and their coordination mechanism by EXAFS measurement using novel hybrid adsorbent, Chemical Engineering Journal 225 (2013) 558–566;
(b) M.R. Awual, T. Kobayashi, Y. Miyazaki, R. Motokawa, H. Shiwaku, S. Suzuki, Y. Okamoto, T. Yaita, Selective lanthanide sorption and mechanism using novel hybrid Lewis base (N-methyl-N-phenyl-1,10-phenanthroline-2-carboxamide) ligand modified adsorbent, Journal of Hazardous Materials 252–253 (2013) 313–320;
(c) M.R. Awual, T. Yaita, H. Shiwaku, Design a novel optical adsorbent for simultaneous ultra-trace cerium(III) detection, sorption and recovery, Chemical Engineering Journal 228 (2013) 327–335.
[27] E. Palomares, R. Vilar, A. Green, J.R. Durrant, Alizarin complexone on nanocrystalline TiO_2: a heterogeneous approach to anion sensing, Advanced Functional Materials 14 (2004) 111–115.
[28] (a) M.R. Awual, T. Yaita, S.A. El-Safty, H. Shiwaku, S. Suzuki, Y. Okamoto, Copper(II) ions capturing from water using ligand modified a new type mesoporous adsorbent, Chemical Engineering Journal 221 (2013) 322–330;
(b) M.R. Awual, T. Yaita, Rapid sensing and recovery of palladium(II) using *NN*-bis(salicylidene)1,2-bis(2-aminophenylthio)ethane modified sensor ensemble adsorbent, Sensors and Actuators B: Chemical 183 (2013) 332–341.
[29] (a) M.R. Awual, T. Yaita, S.A. El-Safty, H. Shiwaku, Y. Okamoto, S. Suzuki, Investigation of palladium(II) detection and recovery using ligand modified conjugate adsorbent, Chemical Engineering Journal 222 (2013) 172–179;
(b) M.R. Awual, M. Ismael, M.A. Khaleque, T. Yaita, Ultra-trace copper(II) detection and removal from wastewater using novel meso-adsorbent, Journal of Industrial and Engineering Chemistry (2013), http://dx.doi.org/10.1016/j.jiec.2013.10.009;
(c) M.R. Awual, S. Suzuki, T. Taguchi, H. Shiwaku, Y. Okamoto, T. Yaita, Radioactive cesium removal from nuclear wastewater by novel inorganic and conjugate adsorbents, Chemical Engineering Journal 242 (2014) 127–135.
[30] (a) M.R. Awual, I.M.M. Rahman, T. Yaita, M.A. Khaleque, M. Ferdows, pH dependent Cu(II) and Pd(II) ions detection and removal from aqueous media by an efficient mesoporous adsorbent, Chemical Engineering Journal 236 (2014) 100–109;
(b) M.R. Awual, M. Ismael, T. Yaita, Efficient detection and extraction of cobalt(II) from lithium ion batteries and wastewater by novel composite adsorbent, Sensors and Actuators B: Chemical 191 (2014) 9–18.
[31] M.J. Frisch, et al., Gaussian 03, Revision C.01, Gaussian, Inc, Wallingford, CT, 2004.

[32] R. Ditchfield, W.J. Hehre, J.A. Pople, Self-consistent molecular orbital methods. IX. An extended gaussian type basis for molecular orbital studies of organic molecules, The Journal of Chemical Physics 54 (1971) 724–728.
[33] P.J. Hay, W.R. Wadt, Ab initio effective core potentials for molecular calculations. Potentials for the transition metal atoms Sc to Hg, The Journal of Chemical Physics 82 (1985) 270–283.
[34] K. Takahashi, Crystal structure of the gold(III) complex, trichloro(dibenzyl sulfide)gold(III), Bulletin of the Chemical Society of Japan 64 (1991) 2572–2574.
[35] K.D. Sen, D.M.P. Mingos, Structure and Bonding Chemical Hardness, vol. 80, Springer, Berlin, 1993.
[36] R.G. Parr, W. Yang, Density Functional Theory of Atoms and Molecules, Oxford University Press, Oxford, 1989.
[37] P. Geerlings, F. de Proft, W. Langenaeker, Conceptual density functional theory, Chemical Reviews 103 (2003) 1793–1874.
[38] (a) M.R. Awual, M.A. Shenashen, T. Yaita, H. Shiwaku, A. Jyo, Efficient arsenic(V) removal from water by ligand exchange fibrous adsorbent, Water Research 46 (2012) 5541–5550;
(b) M.R. Awual, S.A. El-Safty, A. Jyo, Removal of trace arsenic(V) and phosphate from water by a highly selective ligand exchange adsorbent, Journal of Environmental Sciences 23 (2011) 1947–1954;
(c) M.R. Awual, S. Urata, A. Jyo, M. Tamada, A. Katakai, Arsenate removal from water by a weak-base anion exchange fibrous adsorbent, Water Research 42 (2008) 689–696;
(d) M.R. Awual, A. Jyo, Rapid column-mode removal of arsenate from water by crosslinked poly(allylamine) resin, Water Research 43 (2009) 1229–1236.
[39] (a) M.R. Awual, A. Jyo, T. Ihara, N. Seko, M. Tamada, K.T. Lim, Enhanced trace phosphate removal from water by zirconium(IV) loaded fibrous adsorbent, Water Research 45 (2011) 4592–4600;
(b) M.R. Awual, A. Jyo, Assessing of phosphorus removal by polymeric anion exchangers, Desalination 281 (2011) 111–117;
(c) M.R. Awual, M.A. Hossain, M.A. Shenashen, T. Yaita, S. Suzuki, A. Jyo, Evaluating of arsenic(V) removal from water by weak-base anion exchange adsorbents, Environmental Science and Pollution Research 20 (2013) 421–430;
(d) M.R. Awual, A. Jyo, S.A. El-Safty, M. Tamada, N. Seko, A weak-base fibrous anion exchanger effective for rapid phosphate removal from water, Journal of Hazardous Materials 188 (2011) 164–171;
(e) M.R. Awual, M.A. Shenashen, A. Jyo, H. Shiwaku, T. Yaita, Preparing of novel fibrous ligand exchange adsorbent for rapid column-mode trace phosphate removal from water, Journal of Industrial and Engineering Chemistry (2013), http://dx.doi.org/10.1016/j.jiec.2013.11.016.
[40] C.P. Gomes, M.F. Almeida, J.M. Loureiro, Gold recovery with ion exchange used resins, Separation and Purification Technology 24 (2001) 35–57.
[41] M. Cox, A.A. Pichugin, E.I. El-Shafey, Q. Appleton, Sorption of precious metals onto chemically prepared carbon from flax shive, Hydrometallurgy 78 (2005) 137–144.

Biographies

Md. Rabiul Awual received his bachelor (Hons) and MSc from the Department of Applied Chemistry and Chemical Technology, University of Dhaka, Bangladesh. He obtained the PhD degree in industrial and environmental science and engineering in 2008 (Kumamoto University, Japan). In 2009, he was appointed as an analytical manager in Bureau Veritas Consumers Products Services (BD) Ltd. He also worked as visiting scientist in Pukyong National University, South Korea. In 2010, he awarded NIMS Researcher fellowship and conducted the research successfully for two years. He is the author of dozens of scientific articles published in reputed international journals. He is currently appointed a fixed-term researcher at Japan Atomic Energy Agency (JAEA), Japan. His research activity has covered a wide range of novel material preparation and coordination with metals ions specifically lanthanide and actinide, adsorbent materials for specific functional groups and environmental applications.

Mohamed Ismael received his PhD degree in 2009 from Tohoku University, Japan in major of applied chemistry. He worked at National Institute for materials Science (NIMS) as post-doctoral fellow. He is currently a lecturer in Sohag University, Egypt. His research interest is focusing in modeling designs based theoretical chemistry for nanostructured organic–inorganic hybrid materials, biomaterials and polymers.